Proc. Lunar Planet. Sci. Conf. 11th (1980), p. 1855–1865.
Printed in the United States of America

Focal mechanism of deep moonquakes

Junji Koyama* and Yosio Nakamura

Marine Science Institute, Geophysics Laboratory, University of Texas, Galveston, Texas 77550

Abstract—To elucidate the focal mechanism of deep moonquakes, we analyzed S-wave polarizations of deep moonquake signals from the A_1 source region. At station 12, where the available data are of the highest quality, the variation of polarization angle with the anomalistic phase of the moon indicates agreement with that expected from the focal mechanism model of Nakamura. Focal mechanism solutions were derived for eight A_1 moonquakes assuming that moonquakes are, like earthquakes, caused by a shear fracture on a fault plane. The mechanism solutions generally indicate a nearly horizontal or almost vertical faulting. The slip directions estimated from the solutions are different from one another, again suggesting variation of focal mechanisms as a function of the tidal phase of the moon.

INTRODUCTION

Two distinct types of moonquakes which have been identified so far are deep moonquakes (Latham *et al.*, 1971) and shallow moonquakes (Nakamura *et al.*, 1974). Deep moonquakes, which are numerous but small, exhibit several characteristic features: First, they are concentrated mainly at depths between 800 and 1000 km, roughly halfway to the center of the moon. Second, they occur repeatedly in each of a number of distinct source regions, producing groups of seismic signals with nearly identical waveforms. Third, they are closely synchronized with the periodic tides raised on the moon by the earth and the sun. Shallow moonquakes, in contrast, are sparse but relatively large. They are believed to occur at depths shallower than 100 km and show no apparent periodicity in their activity (Nakamura *et al.*, 1979).

The most active group of deep moonquakes, designated A_1, includes 187 events detected between 1969 and 1977, among which are many of the largest deep moonquakes ever observed. Some of the A_1 events during 1972 to 1974 showed reversed polarity of seismic signals (Lammlein, 1977; Nakamura, 1978). Toksöz *et al.* (1977) and Cheng and Toksöz (1978) compared the calculated tidal stresses in a moon model with the occurrence of A_1 moonquakes, and concluded that the presence of a constant ambient tectonic stress is necessary to explain the observed reversal in the polarities of A_1 moonquake signals.

* Present address: Geophysical Institute, Faculty of Science, Tohoku University, Sendai 980, Japan

On the other hand, Nakamura (1978) analyzed the variation of amplitude ratios of P and S waves generated by A_1 moonquakes and showed that the mechanism at the source is not just a reversal of motion as suggested by the Toksöz model, but a rotation of slip vector controlled by the shifting tidal stress field. He consequently suggested that deep moonquakes are the manifestation of mere storage and release of tidal energy within tectonically-inactive lunar interior.

In order to learn more about the focal mechanism of deep moonquakes, we looked for further clues in the properties of S-waves generated by deep moonquakes. We examined polarizations of S waves because they are directly related to the focal mechanism, and are an independent source of information relative to both P wave polarities and amplitude ratios of P and S waves previously analyzed (Lammlein, 1977; Chen and Toksöz, 1978; Nakamura, 1978).

METHOD OF ANALYSIS

Focal mechanisms of earthquakes are usually studied by analyzing polarities of P-wave first motion and/or directions of S-wave initial motions (Honda, 1962). However, the complexity of lunar seismic signals due to intensive scattering and the paucity of seismic stations on the moon preclude the application of these conventional analysis techniques. The method used in this study is to evaluate the directions of particle motion of S waves in a statistical manner.

Let the observed seismic signal around the S-wave onset time be given as a set of discrete time series x_i and y_i on two horizontal orthogonal coordinates (x, y) of the instrument. (The Apollo lunar seismometers use left-handed coordinate system with the positive z-axis pointing upward. The orientations of horizontal axes are given in the caption for Table 1). The signals can also be expressed in another set of time series X_i and Y_i on a horizontal coordinate system (X, Y) which is rotated by an angle α with respect to (x, y). The correlation coefficient r between the components X_i and Y_i is defined by

$$r^2 = E(X \cdot Y)^2 / E(X^2)E(Y^2), \tag{1}$$

where E(X) denotes the mathematical expectation of X. It is assumed that the means of X_i and Y_i are zero; i.e., dc components have been removed from the signal. The correlation coefficient r vanishes when X and Y axes are the major and minor axes of the orbital motions of S waves. Then, the angle α is given as a solution of $E(X \cdot Y) = 0$, i.e.,

$$\tan \alpha = \{ D \pm \sqrt{D^2 + S_{xy}^2} \} / S_{xy}, \tag{2}$$

where $S_{xy} = E(x \cdot y)$, $D = (S_{yy} - S_{xx})/2$, $S_{yy} = E(y^2)$, and $S_{xx} = E(x^2)$.

The plus sign in the numerator corresponds to a rotation in which the X axis coincides with the major axis and the Y axis with the minor axis of the orbital motions of S waves. The use of minus sign places the Y axis on the major, and the X axis on the minor axis. We adopt the former convention in the analysis that follows. Then the angle α becomes the direction of the major axis measured clockwise from the x axis. The ratio of $E(X^2)$ to $E(Y^2)$ gives a measure of ellipticity of the particle orbital motions. We will instead define a linearity coefficient f of the particle motion by

$$f = 1 - \sqrt{E(X^2)/E(Y^2)}, \tag{3}$$

which leads to

$$f = 1 - \sqrt{(S_{yy}\gamma^2 + 2S_{xy}\gamma + S_{xx}) / (S_{xx}\gamma^2 - 2S_{xy}\gamma + S_{yy})}, \tag{4}$$

where $\gamma = (D - \sqrt{D^2 + S_{xy}^2}) / S_{xy}$.

DIRECTION OF S-WAVE ORBITAL MOTIONS

The present analysis was based on A_1 deep moonquakes detected through 1977, the end of the passive seismic experiment of the Apollo project. First, for each seismogram of these moonquakes, a 7.2 second data secton (48 data points) containing the initial S-wave arrival was selected for each of the two horizontal components as indicated by boxed sections in the sample seismograms of Fig. 1. Seismic signals recorded at stations 12 and 15 generally show well defined S-wave

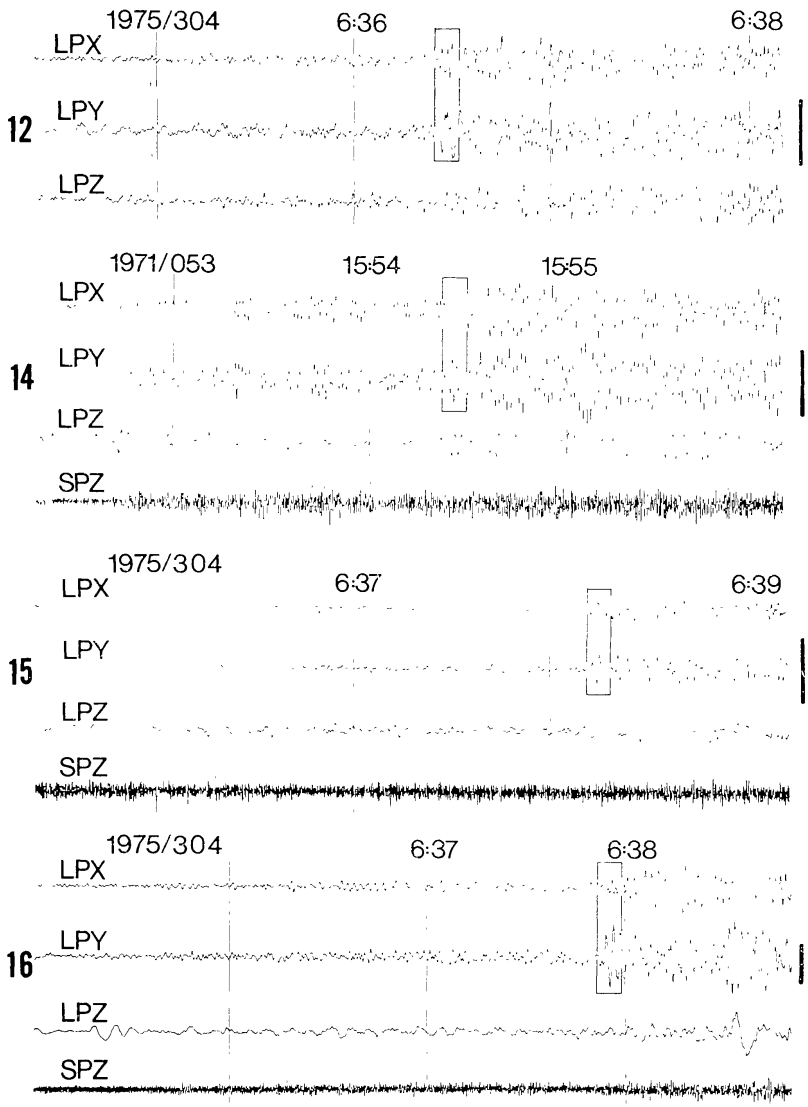

Fig. 1. Seismograms of A_1 deep moonquakes at Apollo seismic stations 12, 14, 15 and 16. LPZ and LPY are long-period horizontal components, and LPZ and SPZ are long- and short-period vertical components, respectively. Signals around S-wave arrivals used for the analysis are indicated in the figure. Except for those of station 14, all seismograms were recorded in the flat-mode response of the seismometers. Vertical bars indicate amplitude of 20 DU, where DU (digital unit) is the unit of signal digitization performed on the moon.

Table 1. Directions of S-wave orbital motions and linearity coefficients. The directions of orbital motions are measured clockwise from the positive x direction of each instrument. The positive x directions are due south, due north, due north, and N25.5°W for stations 12, 14, 15, and 16, respectively.

			Station							
			12		14		15		16	
Year	Day	Time[1]	α	f	α	f	α	f	α	f
1970	9	0203	116°	0.67						
	35	2041	111	.60						
	38	133	104	.55						
	63	424	124	.59						
	64	2344	106	.56						
	91	953	108	.65						
	116	1431	124	.65						
	145	1214	111	.56						
	171	032	134	.54						
	173	1158	115	.56						
	201	1144	114	.65						
	226	1827	125	.57						
	252	1212	117	.52						
	280	549	129	.61						
	284	938	123	.57						
	307	1716	126	.55						
	361	2036	130	.58						
	363	1428	111	.62						
	365	1543	114	.63						
1971	28	1500	115	.61						
	51	1508	138	.60						
	53	1554	129	.63	88°	0.68				
	56	1217	93	.50	110	.53				
	80	1631	130	.61	95	.74				
	82	2115	128	.53	92	.54				
	85	0027			92	.52				
	107	613			88	.50				
	137	537	141	.69	91	.53				
	160	1018	138	.61						
	163	640	120	.65	90	.84				
	187	1655	118	.54	86	.60				
	216	716	133	.60	90	.55				
	218	722	124	.54	89	.82				
	245	2314	127	.57	85	.54	89°	0.70		
	273	2034			92	.53				
1972	17	414	148	.62			88	.53		
	44	2126			91	.72	96	.62		
	164	2349							80°	0.65
1973	20	007							85	.85
	50	1257							82	.72
	60	717	105	.51					100	.62

[1]approximate arrival time of s-wave at station 12

Table 1. *(Continued)*

			Station							
			12		14		15		16	
Year	Day	Time	α	f	α	f	α	f	α	f
1973	88	640			91	.86	123	.56		
	116	1058							86	.73
	127	1908	112	.54	80	.55				
	156	1112	114	.53	84	.67			85	.84
	201	1903	113	.58						
	229	1712	90	.63						
	241	611			89	.56				
	253	1100							76	.67
	270	1747			87°	0.67			101°	0.60
	273	414			94	.81	101°	0.55		
	303	102			92	.76	121	.50		
	321	731	120°	0.67	91	.55			84	.85
	330	236			91	.67				
1974	124	2213					108	.65	81	.85
	127	1949							85	.80
	151	1150	153	.56	91	.59	112	.52	85	.88
	178	2011			89	.57			77	.79
	343	2349			91	.77	119	.65	80	.71
1975	86	1849	105	.52			60	.63	88	.84
	113	1155	119	.54			89	.52	84	.87
	140	1730	118	.57					89	.81
	168	2230	106	.58					88	.85
	250	952	107	.66					87	.74
	276	624	119	.52					88	.72
	278	747	107	.52					93	.56
	304	636	116	.52					86	.71
	331	612							87	.75
1976	20	930	126	.54					91	.66
	76	006			87	.54			94	.71
	102	1604							66	.65
	157	052			94	.74				
	184	122			92	.81			90	.76
	210	1755			90	.84			87	.70
	238	1427							87	.72
	264	1653							83	.72
	266	2019							89	.71
	293	123							88	.76
	294	1937							84	.65
	297	136							87	.67
	320	1500							82	.69
	324	2241							80	.56
	351	1318			91	.78			87	.63
1977	12	700							95	.54
	63	1221			103	.56			85	.67
	65	1019			89	.57			87	.61
	91	1739							88	.63

Table 1. *(Continued)*

			Station							
			12		14		15		16	
Year	Day	Time	α	f	α	f	α	f	α	f
1977	92	1548	116	.60					80	.78
	118	1330							85	.83
	147	1206							83	.68
	149	1137					90	.70	88	.80
	174	222			96	.67				
	175	1449			85	.75			88	.82
	176	2332							90	.74
	202	1139							86	.83
	229	1651			90	.93			87	.80
	254	1047			88	.68			84	.79
	256	2309			89	.78	97	.56	85	.82

arrivals, while those at stations 14 and 16 are not so well defined but of a ringing nature caused presumably by surface layering at these sites. The time window included 3 to 5 cycles of seismic waves. For each selected section, the angle α of the particle orbital motions of S waves as defined by Eq. (2) and the linearity coefficient f as defined by Eq. (4) were calculated. Table 1 lists the computed values. A blank space indicates either that there are no data, signal amplitudes are too small for the analysis, or that the linearity coefficient is less than 0.5. The linearity coefficient, f, greater than 0.5 means that more than 80% of the wave energy is in the direction of the major axis. Events for which reliable directions could not be determined for any station are not included in the table. The data cover a full period of the six-year tidal periodicity for stations 12 and 14, and successively shorter periods for the later missions, being reduced to 5 years for station 16.

Figure 2 shows directions of S-wave orbital motions at station 12 plotted against the anomalistic phase of the moon at the time of occurrence of each A_1 event. No systematic difference can be found between the flat-mode and peaked-mode data, though the latter data scatters more.

The model by Toksöz *et al.* (1977) involves a simple reversal of slip directions, and thus predicts two discrete values of S-wave polarization angles differing by 180° from each other for all the A_1 moonquakes. Since these two polarization angles would give exactly the same angle α of the S-wave orbital motion, there should be a single constant value of α in Fig. 2. The model by Nakamura (1978), on the other hand, predicts strong dependence of S-wave polarization on the tidal phase of the moon as indicated by the solid curves in Fig. 2. The agreement between the observation and the theory is encouraging. The necessary adjustment of the parameters may indicate that the true coordinates of the A_1 source region are slightly east of the assumed coordinates (14.4°S, 34.0°W), or that local, lateral velocity heterogeneities are affecting the direction of arrivals of seismic rays.

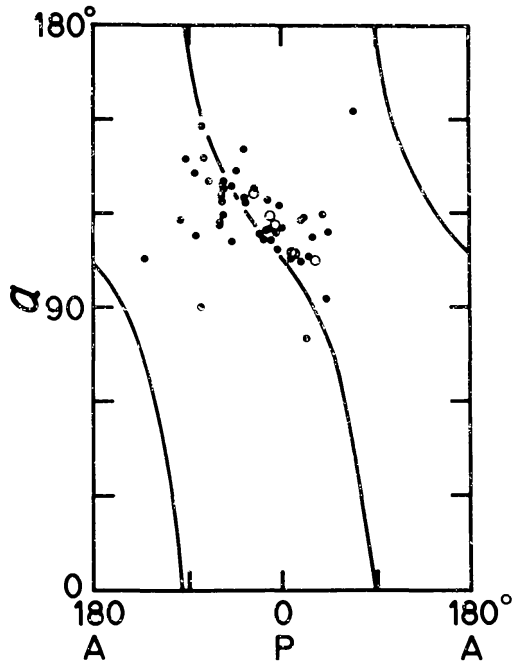

Fig. 2. Directions of S-wave orbital motions at station 12 measured from the positive x coordinate of the instrument. They are plotted against anomalistic phase of the moon at the time of occurrence of each event. A and P represent apogee and perigee, respectively. Open circles indicate those obtained from seismograms in flat-mode response, and solid circles in peaked-mode response. Solid curves in the figure show theoretical directions of S-wave orbital motions derived from the model of focal mechanism for A_1 moonquakes by Nakamura (1978). The adjusted parameters are $\theta = 35°$, $\psi = 100°$ and $A_z = 200°$, where θ is the angle between the normal to the fault plane and the line connecting the focus with the station, ψ is the azimuth of the slip direction at perigee relative to the projection of the source-station line on the fault plane and A_z is the azimuth of the epicenter looking from the station. The corresponding parameters of the original model by Nakamura (1978) are $\theta = 28°$, $\psi = 85°$ and $A_z = 222°$.

For stations 14, 15, and 16 (Fig. 3), the agreement between the observations and the theory is poor. The nearly constant directions of S-wave polarization at stations 14 and 16, if taken by themselves, may suggest a simple reversal of slip directions as indicated by the model of Toksöz *et al.* (1977). However, the constant polarization angle at station 14 is clearly inconsistent with those at station 12, which is very close to station 14. Most of the directions at stations 14 and 16 are about 90°, which simply means the initial S-wave amplitudes on the y component are always much larger than those on x components at these stations.

There are some uncertainties about the response of horizontal-component seismometers at these stations. It has long been noted that the y component always shows larger amplitudes than the x component regardless of the source type and source azimuth. There is no indication that actual instrumental gains are different. The discrepancy may be caused by local structural heterogeneities and/or by the way the seismometers are installed on the lunar surface. Since no one knows for sure what causes this discrepancy and especially what would be its effect on initial arrivals such as those used in the present study, we decided not to

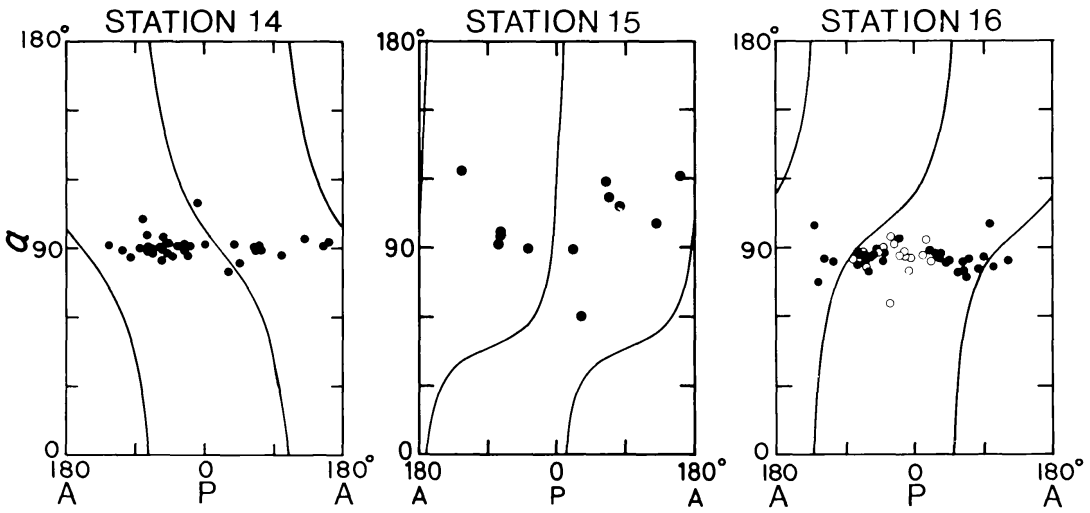

Fig. 3. Directions of S-wave orbital motions at stations 14, 15 and 16. See the caption for Fig. 2 for further explanation.

"correct" for the amplitude differences. Besides, an inspection of sample seismograms in Fig. 1 clearly shows that the difference in the initial S-wave amplitude between x and y components are much more than those of the remainder of the seismograms.

Additionally, for station 14, there is an uncertainty in determining when the shear wave actually arrives. The seismometers at this station could not be operated stably in the flat (wide-band) mode. As a result, there is a possibility that the phase we used is not a real, pure S arrival. Nevertheless, the concentration of the observed polarizations at these stations near 90°, where the theoretical curves have inflections, is encouraging. The large scatter of the data at station 15 is most likely to be due to very small signal amplitudes normally recorded at this station.

FOCAL MECHANISM SOLUTIONS OF A_1 MOONQUAKES

If we assume that moonquakes, like earthquakes, are caused by a shear fracture on a fault plane, we can determine the orientation of the equivalent force system to cause a shear fracture from three observations of polarization angles (Hirasawa, 1966). Three determinations of polarization angles have been made for each of eight events out of 187 A_1 moonquakes. Figure 4 shows the focal mechanism solutions derived for these events. Three solutions exist for most events; however, some of them can be rejected by taking into account the relative polarity relations among seismograms at different stations as given by Nakamura (1978). Since the polarization angles determined in this study do not contain information as to the polarity of S-wave initial motions, it is impossible to tell which of the quadrants represents compression, or rarefaction, for P-wave initial motions.

For those events for which station 14 data are not used, at least one acceptable solution shows a focal mechanism in which one of the nodal planes is nearly vertical and the other horizontal. A typical example is the one for the event of 1975, day 86 in Fig. 4. Although three observations of polarization angles are just enough to determine the orientation of the force system, and despite the fact that polarization angles at some stations may not be as reliable as others and that some of the data may be contaminated by scattered signals, the solutions are fairly close to those postulated by Nakamura (1978) from amplitude ratios of P and S waves. Nakamura (1978) chose the horizontal nodal plane to be the fault plane from the analysis of the relative hypocenter distribution of A_1 moonquakes.

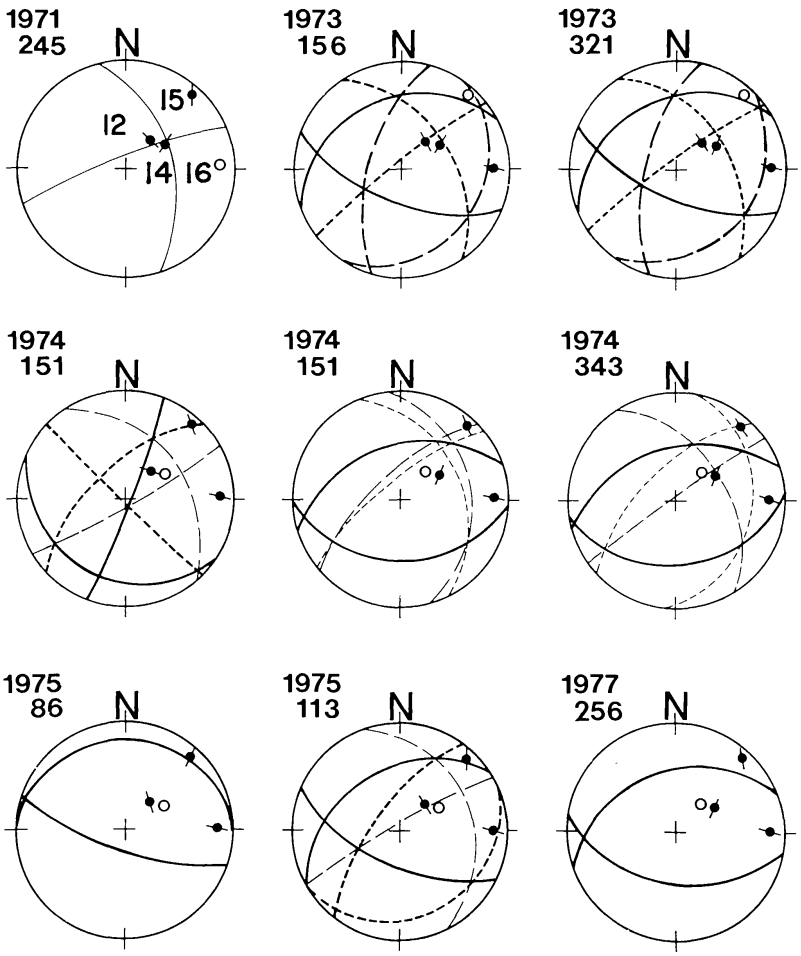

Fig. 4. Focal mechanism solutions for A_1 moonquakes derived from three observations of polarization angles of S-waves. Thick curves indicate sets of two nodal planes of P waves, the fault plane and auxiliary plane, that satisfy the relative polarity relations among seismograms at different stations given in Nakamura (1978). Thin curves indicate those which do not satisfy the polarity relation. They are plotted on the upper hemisphere using equal area net. Solid dots indicate stations used for the solution, each with a line indicating the S-wave polarization angle. Open circles simply indicate locations of other stations not used for the solution. Whether a given quadrant is compressional or dilatational cannot be determined in this solution as explained in the text.

DISCUSSION AND CONCLUSIONS

Two models for the focal mechanism of deep moonquakes have been proposed by Toksöz *et al.* (1977) and Nakamura (1978). The former postulates a combination of the cyclic tidal stresses and a constant ambient tectonics stress to produce moonquakes when tidal unloading allows slippage to occur in one of two opposite directions. The latter postulates a slippage on a horizontal fault plane in a direction that rotates with the tidal phase of the moon. Although both of the models assume a priori a shear fracture as the focal mechanism, these two models lead to quite different concepts of the focal process of deep moonquakes; one is a fracture involving tectonic stress as in earthquakes, and the other is a fracture due to fatigue by cyclic tidal loading.

To clarify this situation, we have analyzed S-wave orbital motions generated by A_1 deep moonquakes. The observed directions of S-wave orbital motions at station 12 indicate time-dependent characteristics of focal mechanisms for A_1 moonquakes in agreement with the results by Nakamura (1978). Although the directions of S-wave orbital motions at other stations may be less reliable than those at station 12, the polarizations of S waves generally agree with those expected for a shear fracture on a fault.

Focal mechanism solutions were derived for eight A_1 events, assuming that moonquakes, like earthquakes, are caused by shear fracture. Most of the solutions show a mechanism of nearly horizontal or almost vertical faulting, which is in agreement with the one postulated by Nakamura (1978) from the amplitude ratio of P and S waves. Because of the paucity of observations, the mechanism solutions are not so constrained as to be unique; however, the mechanisms are different from one another, again suggesting temporal variation of the slip direction on the fault. The variation sometimes results in a reversal of polarity of A_1 seismograms at certain stations.

Our current thinking on the focal mechanism of deep moonquakes may be summarized as follows. Toksöz *et al.* (1977) first postulated a mechanism model just to explain the polarity reversal of seismograms at certain stations. Later, Nakamura (1978) showed that a different model was needed to explain several other aspects of the observed data. These two models are not necessarily mutually exclusive in all respects. In fact, many features of the models are common, including an existence of nearly horizontal fault planes and the dominant role played by the tidal stress. Nakamura's observation indicates that it is not necessary to have accumulated tectonic stress for the deep moonquakes to occur there. A small amount of tectonic stress may be present, but it cannot play a dominant role without contradicting the observed amplitude variations. Thus we have a model in which the tidal effects play a major role both in supplying the necessary strain energy and some mechanisms to initiate moonquakes. The study reported here gives a support to such a model by showing the observed shear wave polarizations are also in agreement.

The maximum shear stresses induced by tides are less than 1 bar at all depths of a perfectly elastic moon with no small scale heterogeneities (Toksöz *et al.*,

1977; Lammlein, 1977). The magnitude of shear stress in such a moon is dependent on the shear modulus profile in its interior. However, the shear stress reaches a maximum around the depths of deep moonquake sources irrespective of assumed lunar structure. Toksöz *et al.* (1977) estimated the magnitude of ambient tectonic stress to be about 0.5 bar for the polarity reversal of seismograms of A_1 moonquakes. These stress levels are far below the fracture strength of most materials. Fatigue cracking is more likely as the focal process of deep moonquakes under low-stress, cyclic tidal loading. Though calculated tidal stresses based on elastic moon models do not show a sign reversal in any stress components, fatigue cracks are non-linear processes and it is conceivable that polarity reversals in A_1 moonquake seismograms do represent such a process. Some suggestions come from experimental studies of acoustic emissions. Acoustic emissions are observed for rock samples under uniaxial load not only during loading but also during unloading of the sample (Khair, 1977). The rotation of slip directions may be a result of similar non-linear processes under varying tidal stresses.

Acknowledgments—We would like to thank several staff members of the Galveston Geophysics Laboratory, including Drs. Cliff Frohlich, James Dorman and Gary Latham for stimulating discussions during the course of this study and for reviewing the manuscript. This research was supported by NASA Grant NSG-7418, and is University of Texas Marine Science Institute Contribution No. 437, Galveston Geophysics Laboratory.

REFERENCES

Cheng C. H. and Toksöz M. N. (1978) Tidal stresses in the moon. *J. Geophys. Res.* **83,** 845–855.

Hirasawa T. (1966) A least squares method for the focal mechanism determination from S wave data; Part 1. *Bull. Earthq. Res. Inst., Tokyo Univ.,* **44,** 901–918.

Honda H. (1962) Earthquake mechanism and seismic waves. *Geophys. Notes, Tokyo Univ.* **15** Suppl., 1–97.

Khair A. W. (1977) A study of acoustic emission during laboratory tests on Tennessee sandstone. In *Proc. 1st Conf. Acoustic Emission/Microseismic Activity* (H. R. Hardy and F. W. Leighton, eds.), p. 57–86. Trans Tech Publ., Clausthal, Germany.

Lammlein D. R. (1977) Lunar seismicity and tectonics. *Phys. Earth Planet. Inter.* **14,** 224–273.

Latham G., Ewing M., Press F., Sutton G., Dorman J., Nakamura Y., Toksöz N., Duennebier F., and Lammlein D. (1971) Passive seismic experiment. NASA SP-272, p. 133–161.

Nakamura Y. (1978) A_1 moonquakes: Source distribution and mechanism. *Proc. Lunar Planet. Sci. Conf. 9th,* p. 3589–3607.

Nakamura Y., Dorman J., Duennebier F., Ewing M., Lammlein D., and Latham G. (1974) High-frequency lunar teleseismic events. *Proc. Lunar Sci. Conf. 5th,* p. 2883–2890.

Nakamura Y., Latham G., Dorman J., Ibrahim A., Koyama J., and Horvath P. (1979) Shallow moonquakes: Depth, distribution and implications as to the present state of the lunar interior. *Proc. Lunar Planet. Sci. Conf. 10th,* p. 2299–2309.

Toksöz M. N., Goins N. R., and Cheng C. H. (1977) Moonquakes: Mechanisms and relation to tidal stresses. *Science* **196,** 979–981.